Thermal expansion studies of superconducting $U_{1-x}Th_xBe_{13}$ ($0 \leqslant x \leqslant 0.052$): Implications for the interpretation of the T-x phase diagram

F. Kromer, M. Lang, N. Oeschler, P. Hinze, C. Langhammer, and F. Steglich
Max Planck Institute of Chemical Physics of Solids, D-01187 Dresden, Germany

J. S. Kim and G. R. Stewart
Department of Physics, University of Florida, Gainesville, Florida 32661

(Received 30 May 2000)

We report on high-resolution measurements of the coefficient of thermal expansion α of the heavy-fermion superconductor $U_{1-x}Th_xBe_{13}$ for temperatures $0.05\,\mathrm{K} \leqslant T \leqslant 6\,\mathrm{K}$ and magnetic fields $B \leqslant 8$ T. Particular attention is paid to the properties of the low-temperature normal state and their evolution as a function of thorium concentration. By exploring a wide concentration range, $0 \leqslant x \leqslant 0.052$, that encompasses the region $x_{c1} = 0.019 < x < x_{c2} = 0.045$ where temperature-dependent specific-heat measurements reveal two subsequent phase transitions at $T_{c1} > T_{c2}$, our study discloses features in the T-x plane that have been overseen by all other techniques applied to this system so far: (i) The substitution of uranium by thorium in UBe_{13} induces an anomaly that manifests itself in a negative $\alpha(T)$ contribution to the low-temperature normal-state expansivity. Its distinct field dependence signals a magnetic origin. Analyzing the relative lengths changes associated with this anomaly and that of the phase transition at T_{c2} suggests a common (presumably magnetic) nature of both features. (ii) The linear concentration dependence of the second low-energy scale $T_{\max}$, which gives rise to a pronounced maximum in $\alpha(T)$ of UBe_{13} at 2 K (at $B=0$) could be followed up—by applying a magnetic field—to concentrations $x > 0.03$. Most remarkably, $T_{\max}(x)$ vanishes at $x \approx 0.043$, i.e., almost exactly at x_{c2}. (iii) Upon increasing x to above 0.03 the normal- to superconducting-state transition at T_{c1} progressively loses its signatures in α. Our measurements, together with recent specific-heat results by Schreiner *et al.* [Schreiner *et al.*, Europhys. Lett. **48**, 568 (1999)] indicate that superconductivity becomes gapless for $x \to x_{c2}$. Hence, the phase transition seen in specific heat as well as thermal-expansion measurements for samples with $x > x_{c2}$ has to be attributed to the T_{c2} transition. Concomitant investigations of the ac susceptibility indicate that the normal- to superconducting-state transition for $x > x_{c2}$ now coincides with T_{c2}. As for the implications of our observations for the interpretation of the various low-temperature anomalies, we discuss two possible scenarios both of which imply an intimate interrelation of superconductivity with the symmetry broken state that forms below T_{c2}.

I. INTRODUCTION

The heavy-fermion (hf) superconductor UBe_{13} (Ref. 1) and its Th-doped homologues are distinct by showing most complex behaviors both above and below T_c. For the pure compound a characteristic (Kondo) scale of $T^* \approx 8-25\,\mathrm{K}$, which accounts for the extremely large effective carrier masses, has been inferred from specific-heat[2] and resistivity measurements.[3] In addition to this predominant energy scale, yet another low-temperature scale has been found that manifests itself in maxima centered around $T_{\max} = 2\,\mathrm{K}$ in thermodynamic[4–6] and transport properties.[1,3,7]

Furthermore, the low-temperature normal (n)-state properties are characterized by strong violations of Landau-type Fermi-liquid behavior. In fact, a closer inspection of the resistivity and specific heat supports the possibility of a non-Fermi-liquid (nFl) arising from a nearby quantum critical point[8] similar to what was found for the canonical hf superconductor $CeCu_2Si_2$.[9] Unlike the latter, however, where a spin-density-wave (SDW) type magnetic ''phase A'' competes with hf superconductivity,[10,9] no clear-cut evidence for magnetic order exists for UBe_{13} so far.

Out of the highly resistive, strongly incoherent nFl n-state, the superconducting instability evolves at $T_c = 0.9\,\mathrm{K}$.[11] From the T^3 dependence in the low-temperature specific heat, a highly anisotropic, i.e., axial order parameter has been inferred.[14] Even more intriguing was the discovery of a strongly nonmonotonic $T_c(x)$ dependence and the occurrence of a double phase transition in temperature-dependent specific-heat measurements for the thoriated system $U_{1-x}Th_xBe_{13}$ in the low-concentration range $0.019 < x < 0.045$,[15] cf. Fig. 1: After an initial drop with a rather sharp minimum at $x = x_{c1} = 0.019$, T_c rapidly recovers and reaches a local maximum at $x \approx 0.03$. As was observed in the above specific-heat measurements[15] and recently more thoroughly studied,[16] this increase in T_c is accompanied by the occurrence of a second phase transition in the superconducting state. For further thorium addition these two transitions remain distinct up to $x = x_{c2} \approx 0.045$ above which only a single phase-transition anomaly can be resolved in the thermodynamic quantities, cf. Fig. 1.

If the lower of the two transitions at T_{c2} for $0.019 < x < 0.045$ were to be identified as a (second) superconducting one, this would represent clear evidence for the unconventional nature of the superconducting state in $U_{1-x}Th_xBe_{13}$. Unlike UPt_3—the second hf superconductor showing addi-

 ©2000 The American Physical Society

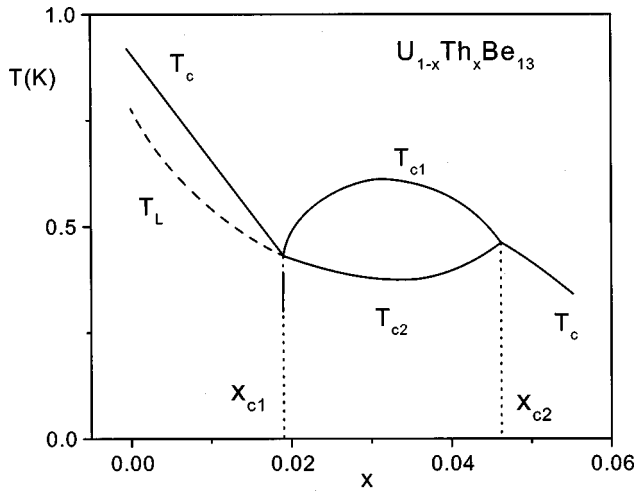

FIG. 1. Schematic T-x phase diagram of $U_{1-x}Th_xBe_{13}$. Full lines represent phase transitions after the recent work of (Ref. 16), while the broken line, $T_L(x)$, corresponds to an anomaly reported in Ref. 17. The existence of an additional phase boundary of second order (vertical solid line) has been inferred from specific-heat measurements under pressure on a sample with $x=0.022$ (Ref. 18). Dotted lines at x_{c1} and x_{c2} define the concentration range in which two subsequent phase transitions at T_{c1} and T_{c2} were found.

tional phase-transition lines below T_c—where compelling evidence exists for multiple superconducting phases (see, e.g., Ref. 19), the situation for $U_{1-x}Th_xBe_{13}$ is not so clear. Here, the problems lie both in the nature of the transition at T_{c2} and—in case it is a second superconducting one—in the cause of the T_c splitting, i.e., the nature of the symmetry-breaking field.

From the marked peak in the ultrasound attenuation below T_{c2}, a spin-density-wave (SDW) ordering was claimed.[20] This was compatible with the increase in the muon spin relaxation (μSR) rate below T_{c2} from which a very small magnetic moment of only $\mu_S \approx 10^{-3}\,\mu_B$/U has been deduced.[21] On the other hand, a second superconducting transition was inferred from the abrupt increase in the slope of the lower critical field upon cooling through T_{c2}.[22] These seemingly conflicting results have been explained by proposing a superconducting state below T_{c2} that breaks time-reversal symmetry.[23–25] More recent experimental results of pressure studies,[18] of the anomalous mixed-state properties,[26,27] and of the response of T_{c2} to doping[28] were found to be consistent with such an interpretation, cf. Ref. 29 for the discussion of the anomalous vortex-pinning phenomena.

The present work comprises a systematic dilatometric study on thoriated UBe_{13} samples for concentrations $0.038 \leqslant x \leqslant 0.052$, i.e., across the second critical concentration x_{c2}, cf. Fig. 1. It supplements our previous study on samples with $x \leqslant 0.03$.[17] The work is aimed at (i) finding out systematics as a function of x that may help to identify the various phases and phase transitions as well as (ii) looking for potential correlations of these states with properties above T_c. As demonstrated in previous thermal-expansion studies[30,5,17] dilatometry has proved to be particularly suited for this purpose owing to the strong coupling of the low-temperature electronic properties to the lattice degrees of freedom.

The paper is organized as follows: After presenting some details concerning experimental techniques and the samples investigated in Sec. II, we present in Sec. III a thorough investigation of the low-temperature thermal expansion and ac susceptibility as well as a comparison to specific-heat data. The results are analyzed in Sec. IV with regard to various aspects. The implication of our findings for the interpretation of the various phases and phase-transition lines are discussed in Sec. V. The paper is summarized in Sec. VI.

II. EXPERIMENTAL

Thermal-expansion measurements were performed utilizing a high-resolution capacitance dilatometer whose maximum sensitivity corresponds to $\Delta l/l = 10^{-11}$ where l is the sample length.[31] The linear coefficient of thermal expansion $\alpha = l^{-1} \times \partial l/\partial T$ is approximated by $\alpha(T) \approx [\Delta l(T_2) - \Delta l(T_1)]/[l(300\,\mathrm{K})(T_2 - T_1)]$, with a mean temperature $T = (T_1 + T_2)/2$ and length changes defined as $\Delta l(T) = l(T) - l(0.05\,\mathrm{K})$. For a determination of the superconducting transition temperatures of our samples an ac susceptometer operating at a frequency $\omega = 117$ Hz was employed. The peak-to-peak amplitude of the ac field was set to $\Delta B = 13\,\mu$T except for the $x = 0.043$ compound, where an amplitude of $\Delta B = 1.05\,\mu$T was used. Since the low-temperature flank of the χ_{ac} transition (but not the onset) was found to depend on the ac-field amplitude, we refrained from using the standard 10–90 % criterion for the determination of T_c. Instead, we used the amplitude-independent nucleation temperature defined as the intercept of the linear extrapolations of $\chi_{\mathrm{ac}}(T)$ from the n-state and from the temperature range of maximum slope below the transition. The specific-heat measurements for the samples with $x = 0$ and $x = 0.03$ were conducted in our laboratory utilizing a thermal-relaxation technique.[32,33] The $C(T)$ data for all other Th concentrations were taken from Refs. 16, 34, 35, where samples cut from the same batches as those investigated here were studied.

While for the pure UBe_{13} single crystalline material was used, all Th-doped samples are polycrystals. Except $U_{0.962}Th_{0.038}Be_{13}$ where both an annealed and unannealed sample was measured all other samples are unannealed. For details on the sample preparation we refer to Ref. 16.

III. RESULTS

Below we present results of thermal-expansion measurements on thoriated UBe_{13} samples with Th concentrations $x = 0.038$, 0.043, 0.0455, and 0.052. This study supplements our recent work which was focusing on the concentration range $x \leqslant 0.03$.[17] The salient results of that work are summarized in Fig. 2 where we plot the thermal-expansion data together with results of the specific heat on the same temperature scale. Starting with the pure compound, the projection of the width of the superconducting transition (vertical dotted lines) from $C(T)$ (upper curves) on to the $\alpha(T)$ data (lower curves) reveals that besides the superconducting transition that manifests itself in the negative jump in $\alpha(T)$ an additional broad negative anomaly shows up slightly below T_c. The independent character of both features has been clearly demonstrated by both their distinctly different field dependences as well as a thorough thermodynamic

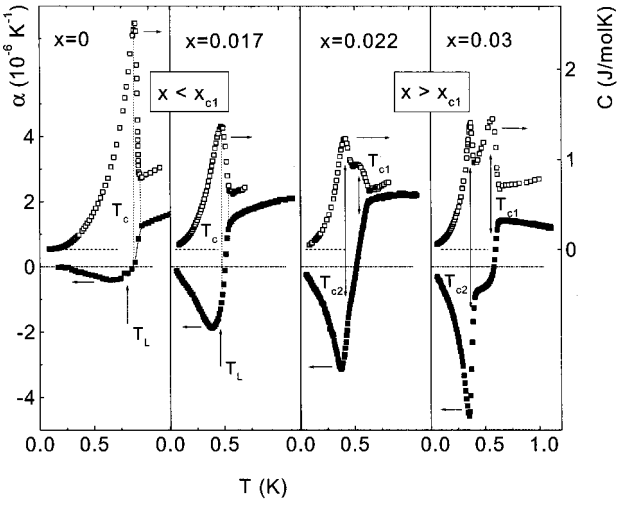

FIG. 2. Low-temperature specific heat (open symbols, right scale) and thermal expansion (closed symbols, left scale) on UBe_{13} single crystal and polycrystalline $U_{1-x}Th_xBe_{13}$ with $x=0.017$, 0.022, and 0.03. The specific-heat data for $x=0.017$ and 0.022 are taken from Refs. 34 and 16, respectively. The width of the superconducting transition for $x=0$ and 0.017 is indicated by the dotted vertical lines. Arrows for $x=0.022$ and 0.03 mark the positions of the phase transitions at T_{c1} and T_{c2}. T_L indicates the position of the negative $\alpha(T)$ anomaly reported in Ref. 17, cf. text.

analysis.[17] Upon increasing x to 0.01 (not shown, cf. Ref. 17), 0.017, and 0.0185 (also not shown, cf. Ref. 36) this low-T feature becomes progressively more pronounced and sharper. Once x is increased to 0.022, i.e., above $x_{c1}=0.019$, the superconducting transition separates on the temperature axis from the low-T anomaly that now receives the character of a true phase transition. Using an equal-areas construction to replace the broadened phase transitions by idealized sharp ones, the transition temperatures can be determined and associated with T_{c1} and T_{c2} in accordance with literature results.[15,21,16] The main observation of our previous study contained in Fig. 2 is that the low-T anomaly for $x<x_{c1}$ in the superconducting state marks the precursor of the transition at $T_{c2}(x)$ for $0.019<x<0.045$. To determine the position of this anomaly as a function of x, we treat, for lack of any other well-founded criterion, the broadened features in the same way as the second-order phase transitions at T_{c2} for $x>x_{c1}$ and refer to their characteristic temperature as $T_L(x)$, cf. Fig. 2.

Before discussing the results for $x>0.03$ in detail, we present in Fig. 3 a compilation of these data together with specific-heat results in the same way as in Fig. 2 for $x\leqslant 0.03$. In addition, Fig. 3 comprises results of ac susceptibility measurements serving as an independent determination of T_{c1}.

By following the evolution of the low-temperature $\alpha(T)$ behavior as a function of Th concentration in Figs. 2 and 3, three observations can be made.

(1) The thermal-expansion coefficient above T_{c1} changes sign from a large positive expansivity for $x\leqslant 0.03$ (cf. also Fig. 2) to a negative one for $x\geqslant 0.038$. The magnitude of the latter contribution, $|\alpha_n|$, grows with increasing x from 0.038 to 0.043 but appears to saturate for higher Th concentrations. Remarkably enough, in the same concentration range, no significant change can be resolved in the corresponding n-state specific heat.

(2) The discontinuity at the superconducting transition at T_{c1} in both thermodynamic quantities becomes strongly reduced upon increasing x to above 0.03. While for $x=0.038$ a somewhat reduced though still sizable $\Delta C|_{Tc1}$ is found together with a $\Delta\alpha|_{Tc1}$ that is already very small,[37] both $\Delta C|_{Tc1}$ and $\Delta\alpha|_{Tc1}$ become equally strongly suppressed for $x\geqslant 0.043$. As a consequence, no significant anomaly associated with the T_{c1} transition can be resolved for $x=0.0455$, although the χ_{ac} data clearly indicate a bulk superconducting transition at a temperature $T_c^{\chi}>T_{c2}$, cf. Fig. 3.

(3) Upon increasing x to above 0.03 the separation of the transition temperatures T_{c1} and T_{c2} continuously narrows in agreement with specific heat.[16] For $x=0.052$ where only a single phase-transition anomaly can be resolved, the susceptibility data indicate that this transition coincides with the onset of bulk superconductivity.

Below we give a detailed description of the thermal-expansion results for the various Th concentrations including the data taken in external magnetic fields.

Figure 4(a) displays $\alpha(T,B)$ results on an annealed $U_{0.962}Th_{0.038}Be_{13}$ sample. For comparison the $B=0$ data for an unannealed sample are included. Unlike the case for $x=0.03$ the low-T n-state expansion coefficient of this com-

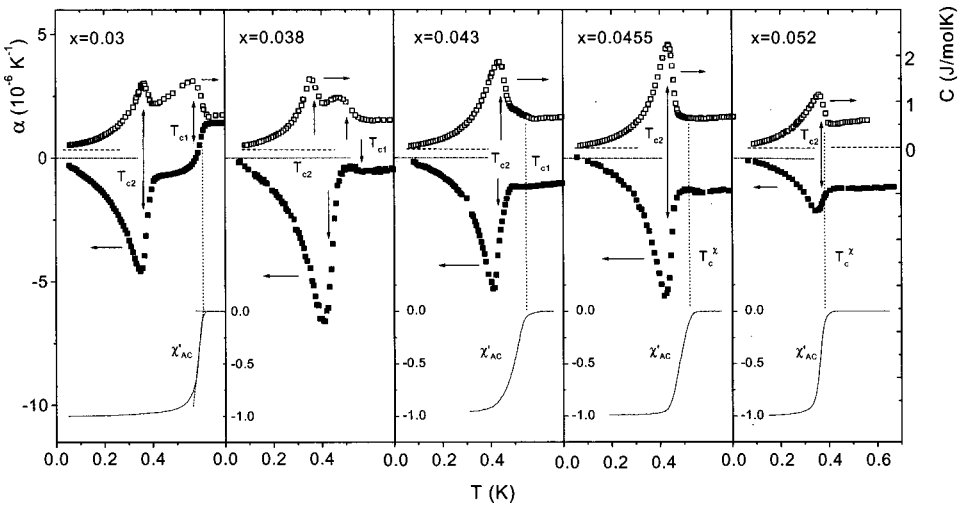

FIG. 3. Low-temperature specific heat (taken from Refs. 16, 35 for $x>0.03$) (open symbols, right outer scale), thermal expansion (closed symbols, left outer scale), and ac susceptibility (solid line, lower inner scale) on polycrystalline $U_{1-x}Th_xBe_{13}$ for varying x. Arrows mark the positions of phase transitions at T_{c1} and T_{c2}. Dotted vertical lines correspond to the superconducting nucleation temperatures the definition of which is described in the text and indicated for $x=0.03$.

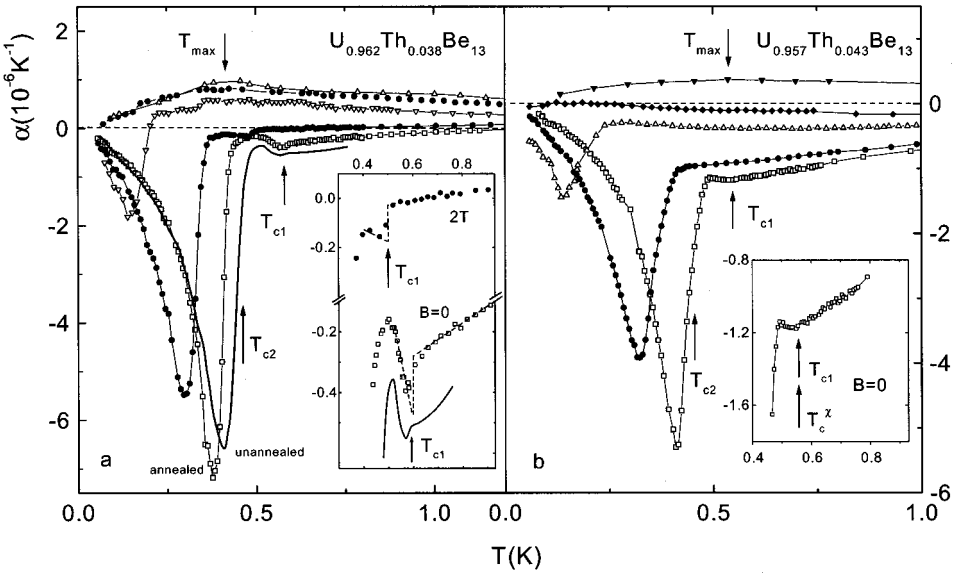

FIG. 4. (a) Coefficient of thermal expansion for an annealed polycrystal $U_{0.962}Th_{0.038}Be_{13}$ in magnetic fields of $B=0$, 2, 4, 6, and 8 T from bottom to top. The thick solid line represent data for an unannealed polycrystal of nominally the same Th concentration. Arrow at T_{max} marks the position of the maximum in $\alpha(T)$ at $B=8$ T. The inset shows the data for the annealed (symbols) and unannealed (solid line) samples close to T_{c1} on expanded scales. Broken lines indicate idealized sharp phase transitions at T_{c1}. (b) Coefficient of thermal expansion on polycrystalline $U_{0.957}Th_{0.043}Be_{13}$ in magnetic fields of $B=0$, 2, 4, 5, and 8 T from bottom to top. The inset magnifies the $B=0$ data around T_{c1}. The arrow at T_c^{χ} marks the position of the superconducting nucleation temperature as defined in the text.

pound is negative at $B=0$. Besides the pronounced phase-transition anomaly at $T_{c2}=438\pm5$ mK only a tiny feature is found at $T_{c1}=580\pm5$ mK. The latter is shown on expanded scales in the inset. Upon increasing the magnetic field both phase-transition anomalies become reduced in size and shifted to lower temperatures. Most remarkably, a distinct field dependence is observed for the negative *n*-state expansivity α_n: upon increasing the field, the negative α_n becomes rapidly suppressed and a somewhat broadened positive peak develops. The data taken at highest fields, i.e., 6 and 8 T indicate that the latter feature almost saturates at this field level and that there is only a weak—if at all—shift in the position of the maximum T_{max}, towards higher temperatures. From these observations we infer that the low-temperature *n*-state $\alpha(T)$ consists of at least two contributions: (i) a strongly field-dependent negative part α_n, superimposed on (ii) a peak structure the position of which is only weakly field dependent in the field range investigated, $B\leqslant 8$ T. The measurements on the unannealed sample of nominally the same Th concentration reveal qualitatively the same behavior [thick solid line in Fig. 4(a)]. It is noteworthy, however, that annealing apparently affects the various low-T features differently: while the anomalous contribution $|\alpha_n|$ as well as the transition temperature T_{c2} are reduced for the annealed sample ($T_{c2}=404\pm5$ mK compared to 438 ± 5 mK for the unannealed sample), the transition at T_{c1} remains virtually unchanged, cf. inset Fig. 4(a).

In Fig. 4(b) we show the results for $U_{0.957}Th_{0.043}Be_{13}$. Compared to the data for $x=0.038$, $|\alpha_n|$ is enhanced for this compound. At the same time both phase-transition anomalies are reduced in size in such a way that at T_{c1} only a break in the slope in $\alpha(T)$ can be resolved. The assignment of the latter feature to the T_{c1} transition is corroborated by ac-susceptibility measurements (cf. Fig. 3) yielding a nucleation temperature T_c^{χ} that coincides with this small $\alpha(T)$ anomaly, cf. inset of Fig. 4(b) [Schreiner *et al.* have previously found a small anomaly in C at T_{c1} for $U_{0.957}Th_{0.043}Be_{13}$ that also corresponds to T_c^{χ} (Ref. 38)]. As for the $x=0.038$ sample we find that with increasing fields the phase-transition anomaly at T_{c2} becomes reduced in size and shifted to lower temperatures. This is accompanied by the suppression of the negative α_n. At the highest field of $B=8$ T a broadened positive peak shows up.

In Fig. 5 we display the data for $U_{0.9545}Th_{0.0455}Be_{13}$—a system that according to Ref. 16 is located very close to the second critical concentration x_{c2}. Following the trend observed for the smaller Th concentrations, a negative α_n is found to dominate the low-temperature *n* state. Further on, only one phase-transition anomaly can be resolved at $T_{c2}=452\pm10$ mK. Figure 5 demonstrates that the superconducting transition, T_{c1}, as indicated by the arrow at T_c^{χ} does not cause any significant response in α. The same holds true for the specific heat, cf. Fig. 3. Applications of a magnetic field cause a reduction of T_{c2} and a suppression of the negative α_n contribution similar to the observations made for the samples with smaller x values. In contrast to the latter, however, no clear maximum structure can be resolved in fields up to 8 T, the highest fields available. A similar behavior is found for $U_{0.948}Th_{0.052}Be_{13}$, cf. Fig. 5(b). The negative α_n is of about the same size as that for the $x=0.0455$ sample [note the different scales in Figs. 5(a) and 5(b)]. Only one phase-transition anomaly at 375 ± 5 mK can be resolved. According to the evolution of the phase-transition anomalies as a function of x for $x\leqslant 0.0455$ (cf. Fig. 3), it is tempting to associate this feature with the T_{c2} transition—an assignment which is also corroborated by specific-heat results,[16] cf. Fig. 3. The measurements of the ac susceptibility indicate that for this

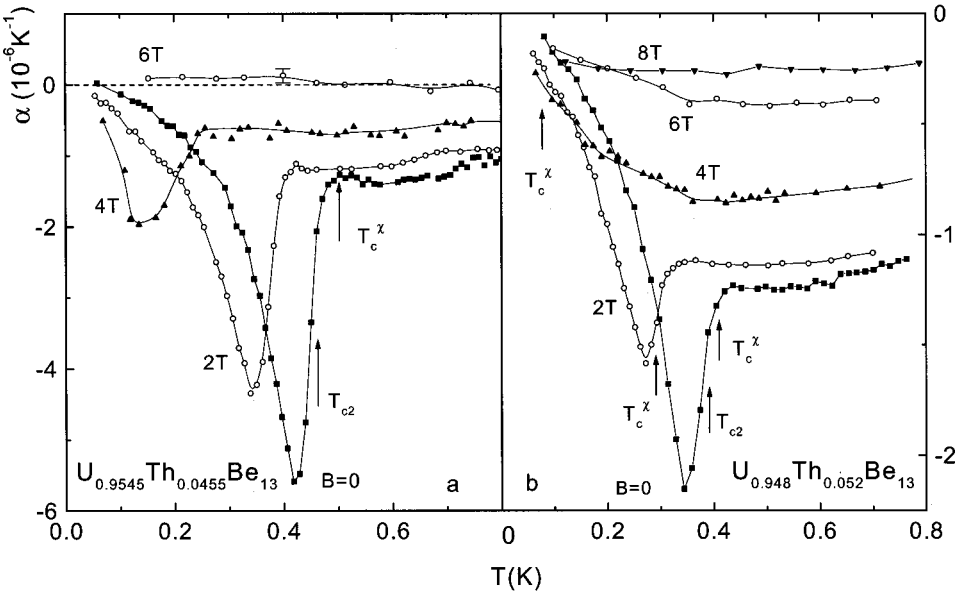

FIG. 5. Coefficient of thermal expansion on polycrystalline $U_{0.9545}Th_{0.0455}Be_{13}$ (a) and $U_{0.948}Th_{0.052}Be_{13}$ (b) at varying magnetic fields. The arrows at T_c^χ mark the positions of the superconducting nucleation temperatures as defined in the text.

concentration T_{c2} almost coincides with the onset of bulk superconductivity at T_c^χ. At a magnetic field of 4 T the signatures of the T_{c2} transition are lost in $\alpha(T,B)$, while χ_{ac} still reveals a superconducting transition at $T_c^\chi(4\,\mathrm{T})=0.1\,\mathrm{K}$ (indicated by the arrow at the 4 T data). Although becoming substantially reduced with increasing field the negative α_n contribution can be resolved up to 8 T for this concentration.

The positions of the phase-transition anomalies in $\alpha(T,B=\mathrm{const})$ and $\chi_{ac}(T,B=\mathrm{const})$ are used to construct B-T phase diagrams for all samples investigated, cf. Fig. 6(b)–6(f). For comparison we show in Fig. 6(a) the B-T diagram of pure UBe_{13} using different scales. Besides the data for the upper critical field, B_{c2}, Fig. 6(a) includes also the positions where anomalies in $\alpha(T,B=\mathrm{const})$ and $C(B,T=\mathrm{const})$ were found[17,36] giving rise to a line of anomalies B^*. This line starts at $T_L\approx 0.7\,\mathrm{K}$ $(B=0)$ and terminates at $B^*\leqslant 5\,\mathrm{T}$.

For thoriated samples inside the concentration range $x_{c1}<x<x_{c2}$ the two transitions remain distinct in magnetic fields but become closer upon increasing the field. A crossing of the phase-transition lines as a function of magnetic field is not observed. For $U_{0.957}Th_{0.043}Be_{13}$ where the T_{c1} transition causes only a minor feature in $\alpha(T)$ [and $C(T)$ (Ref. 38)], its evolution with field can be followed up only for fields $B\leqslant 1\,\mathrm{T}$ above which no significant response is found in $\alpha(T,B)$ anymore. By means of ac susceptibility measurements we were able to follow the superconducting transition temperature to higher fields. While T_c^χ and the transition temperature read off the thermal-expansion data, T_{c1}^α, coincide at $B=0$, they deviate in small fields for reasons which are not known, cf. Fig. 6(e). Most interestingly, Fig. 6(e) suggests that the critical fields of the transitions at T_{c1} and T_{c2} merge in for $T\to 0$. For $U_{0.948}Th_{0.052}Be_{13}$ the field dependence of the phase-transition temperature T_{c2} deduced from thermal-expansion and specific-heat measurements almost coincides with $T_c^\chi(B)$.

Figure 7 compiles in a T-x phase diagram our results on the various anomalies and phase transitions for $U_{1-x}Th_xBe_{13}$.

IV. EVOLUTION OF LOW-TEMPERATURE ANOMALIES AS A FUNCTION OF Th CONCENTRATION

A. Negative thermal-expansion contribution α_n—its possible interrelation with the T_{c2} transition

As demonstrated in Figs. 2 and 3, Th doping not only causes a nonmonotonic $T_c(x)$ dependence accompanied by a double phase transition within a limited x range but also induces anomalies in the n-state properties that are well pronounced in the coefficient of thermal expansion. Two anomalous contributions have been extracted, both of which vary with x: a somewhat broadened and weakly field-

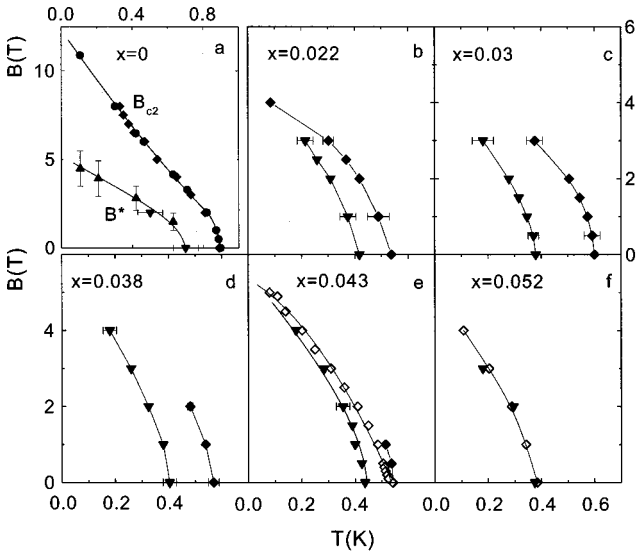

FIG. 6. B-T phase diagrams of $U_{1-x}Th_xBe_{13}$ for varying x. The diagram for UBe_{13} (a) is taken from Ref. 36 (note the different scales). It includes the upper critical field, B_{c2}, and the line of anomalies B^*, as determined by $\alpha(T,B=\mathrm{const})$ (▼) and $C(T=\mathrm{const},B)$ (▲) measurements. (b)–(f) Field dependences of phase-transition anomalies in the coefficient of thermal expansion at T_{c1} (◆) and T_{c2} (▼) as well as superconducting nucleation temperatures T_c^χ (◇) derived from ac susceptibility measurements. The solid lines are guides to the eyes.

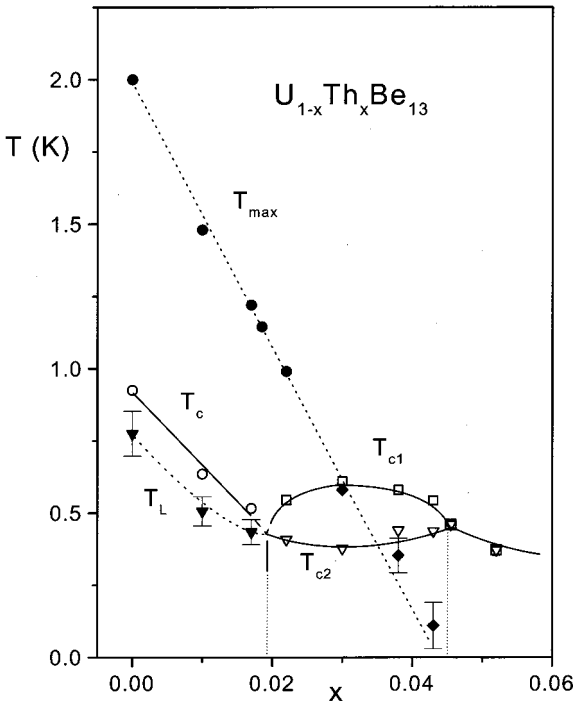

FIG. 7. *T*-*x* phase diagram of $U_{1-x}Th_xBe_{13}$. Open symbols and solid lines indicate phase transitions while closed symbols and broken lines mark anomalies at T_L (▼) and $T_{\max}$ determined from $B=0$ (●) and $B\neq 0$ (◆) data as described in the text. Vertical dotted lines as in Fig. 1.

dependent peak anomaly at $T_{\max}$ besides a strongly field-dependent negative contribution α_n. The latter dominates the low-T n-state expansivity for samples with $x \geqslant 0.038$. To follow its temperature and x dependence we plot in Fig. 8 the $\alpha(T)$ data for some selected Th concentrations over an enlarged temperature range. Upon cooling, the negative contribution gradually grows with an onset temperature around 3 to 4 K that augments with increasing x. Interestingly enough, the data suggest an anticorrelation of this feature with the

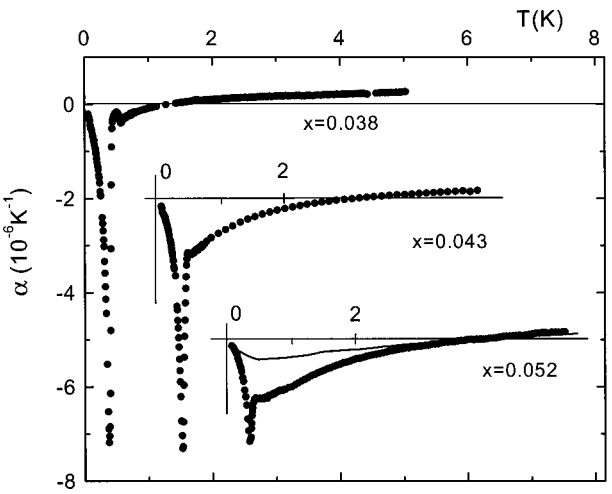

FIG. 8. Coefficient of thermal expansion on polycrystalline $U_{1-x}Th_xBe_{13}$ for $x=0.038$, 0.043, and 0.052 over an extended temperature range. The curves are shifted along both axes for clarity. The data for $x=0.052$ include results taken in $B=6$ T (solid line).

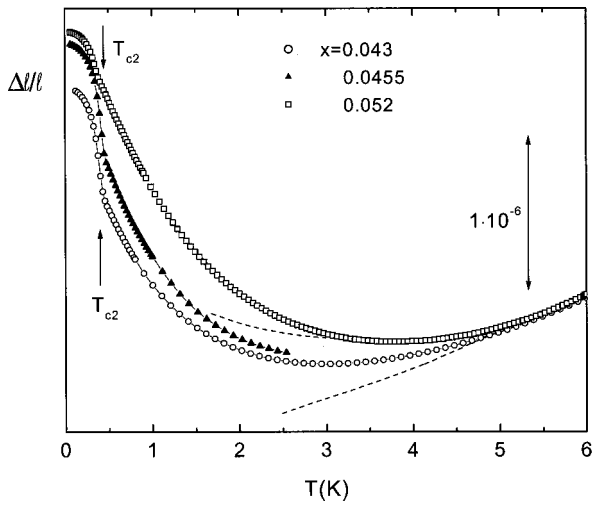

FIG. 9. Relative length changes $\Delta l/l$ vs T of $U_{1-x}Th_xBe_{13}$ for $x=0.043$, 0.0455, and 0.052. The data for $x=0.043$ and 0.052 have been shifted vertically so that they collapse at $T=6$ K (for the $x=0.0455$ data, see text). Broken lines represent the high-temperature part of the data taken in $B=8$ T.

phase transition at T_{c2}: the larger the negative contribution $|\alpha_n|$ the smaller the phase-transition anomaly at T_{c2}. In fact, such an interrelation becomes obvious when plotting the relative length changes, $\Delta l(T)/l$, as a function of temperature for the compounds 0.043, 0.0455, and 0.052, i.e., for systems close to x_{c2} that lack the peak anomaly at $T_{\max}$ in zero magnetic field, cf. Fig. 9. In order to compare the anomalous $\Delta l(T)/l$ contributions for the three compounds on a more quantitative basis, the curves for $x=0.043$ and 0.052 where data up to 6 K are available have been vertically shifted so that they collapse at the high-temperature end. There, the identical slopes of the data indicate a concentration independent $\alpha(T)$ behavior at higher temperatures. For the lack of high-temperature data for $x=0.0455$, the position of the corresponding $\Delta l(T)/l$ curve in Fig. 9 is somehow arbitrary. It can be roughly estimated, however, by considering the slope of the data at highest temperatures being intermediate between the slopes for the $x=0.043$ and 0.052 curves. As indicated for $x=0.043$ and 0.052, the $\Delta l/l$ data taken in magnetic fields of $B=8$ T split off from the $B=0$ curve at elevated temperatures of, respectively, 3 and 5 K, reflecting the strong field dependence of the anomalous upturn in $\Delta l(T)/l$ (negative α_n contribution). The comparison of the $\Delta l(T)/l$ curves in Fig. 9 reveals an overall length change (elongation) upon cooling from 6 K down to 50 mK, the lowest temperature of our experiment, which is similar for the three compounds. Fig. 9 suggests that what happens upon increasing x from 0.043 to 0.0455 and 0.052 is a shift of relative weight of the anomalous $\Delta l(T)/l$ contributions to higher temperatures: an increase of the gradual length change at higher temperatures (negative α_n contribution) at the cost of the rapid elongation associated with the transition at T_{c2}. This observation hints at a common nature of both phenomena—an assignment that is also corroborated by their strikingly similar, strong field response, cf. Figs. 4 and 5. We, therefore, propose that α_n is due to the freezing out of short-range correlations above the long-range ordering at T_{c2}.

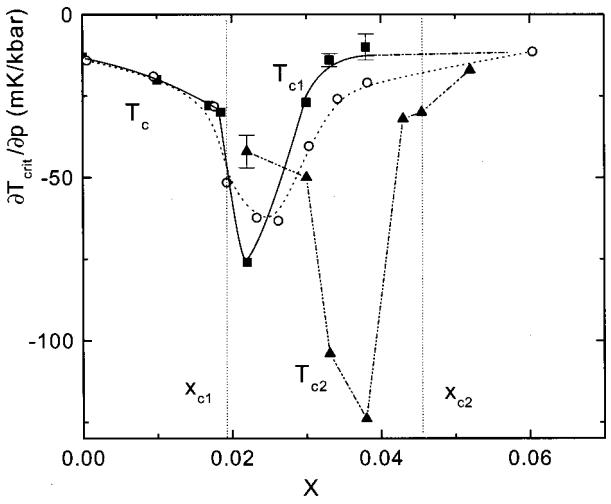

FIG. 10. Pressure dependences of the critical temperature $T_{\rm crit}$ ($=T_c$, T_{c1}, and T_{c2}) vs x. Closed symbols correspond to pressure coefficients derived from the Ehrenfest relation, see text. The corresponding pressure coefficient for $x=0.01$ is taken from Ref. 17, the one for $x=0.0331$ is calculated by using $\Delta\alpha$ and ΔC values read off data shown in Ref. 30. Open circles mark the pressure coefficients of T_c and T_{c1} as read off susceptibility data taken under hydrostatic-pressure conditions in Ref. 40. Vertical dotted lines indicate the critical concentrations x_{c1} and x_{c2}.

B. The normal- to superconducting-state transition at $T_c(x)$ and $T_{c1}(x)$

Following the shape of the phase-transition anomalies in the concentration range where they are well pronounced, i.e., for $0 \leqslant x \leqslant 0.03$, our data do not support the notion of two different types of superconducting phase transitions on both sides of x_{c1}. Rather the $\alpha(T)$ results indicate a common nature of the two transitions, i.e., that $T_c(x)$ connects to $T_{c1}(x)$, and that this $T_c(x)-T_{c1}(x)$ line persists in staying above the $T_L(x)-T_{c2}(x)$ line, cf. Fig. 7. Hence, our thermal-expansion data are inconsistent with a crossing of two phase boundaries as a function of x at x_{c1} that has been discussed by several authors.[23–25] Likewise, no evidence is found for a crossing of the phase boundaries as a function of magnetic field, cf. Fig. 6 and Ref. 39 for $x=0.022$.

C. Hydrostatic-pressure dependences of $T_{c1}(x)$ and $T_{c2}(x)$

Combining the phase-transition anomalies shown in Figs. 2 and 3 at $T_{c1/2}$ in α, $\Delta\alpha_{1/2}$, with those in C, $\Delta C_{1/2}$, via the Ehrenfest relation allows for a determination of the hydrostatic-pressure dependences of $T_{c1/2}$ in the limit of vanishing pressure:

$$\left(\frac{\partial T_{c1/2}}{\partial p}\right)_{p\to 0} = V_{\rm mol}\, T_{c1/2}\, \frac{\Delta\beta_{1/2}}{\Delta C_{1/2}},$$

where for the present cubic systems, the discontinuity in the volume-expansion coefficient $\Delta\beta$ is related to $\Delta\alpha$ via $\Delta\beta_{1/2}=3\Delta\alpha_{1/2}$. For the molar volume we use that of pure UBe_{13} of $V_{\rm mol}=8.13\times10^{-5}\,{\rm cm}^3/{\rm mol}$. The $\Delta\alpha$ and ΔC values for $x=0.0331$ were read off the data shown in Ref. 30. In Fig. 10 we compare the so-derived numbers with the initial pressure coefficients as read off susceptibility data taken under hydrostatic-pressure conditions by Lambert *et al.*[40]. To allow for comparison with the above thermodynamic results for $\partial T_c(x)/\partial p$ and $\partial T_{c1}(x)/\partial p$ we approximate their initial slope, $\partial T_c(x)/\partial p$, by using the $T_c(x)$ curves at $p=0$ and 2 kbars (Fig. 2 of Ref. 40). Except for small differences at concentrations above x_{c1} where $\partial T_{c1}(x)/\partial p$ shows a pronounced minimum, both data sets are in fair overall agreement. Figure 10 demonstrates that Th substitution affects the pressure dependence in a rather nonmonotonic manner: after a smooth initial increase in $|\partial T_c(x)/\partial p|$, the pressure coefficient sharply peaks at a concentration slightly above x_{c1}. For x sufficiently far above x_{c1}—but still below x_{c2}—$|\partial T_{c1}(x)/\partial p|$ drops again to a value close to the one found for $x=0$. Rather than reflecting two different types of superconductivity separated by x_{c1}, as is frequently stated, the above results for $|\partial T_c(x)/\partial p|$ indicate an anomaly that should be associated with a critical Th concentration—most likely x_{c1}.

Figure 10 also includes the pressure coefficient of the transition temperature T_{c2}, $\partial T_{c2}(x)/\partial p$, as calculated by means of the Ehrenfest relation. We find a strong concentration dependence of $|\partial T_{c2}(x)/\partial p|$ with a distinct maximum around $x=0.038$.[41] We note that for $x=0.022$, the above thermodynamic results are at variance with the pressure coefficient inferred from specific-heat measurements performed under uniaxial stress and converted to hydrostatic-pressure units of $\partial T_{c2}/\partial p=-14\pm3$ mK/kbar.[18]

D. The 2 K maximum

The low-temperature n-state expansivity of UBe_{13} is governed by a pronounced peak centered around $T_{\rm max}=2$ K. At the same temperature more or less pronounced maxima are found also in the electrical resistivity[1,42,3,43] and specific heat.[4,6] Via thermal-expansion measurements on thoriated samples with $x\leqslant0.03$, a strictly linear suppression of $T_{\rm max}$ with increasing x was observed.[36] This result is in accordance with the positions of the $C(T)$ maxima reported in Ref. 6. Most interestingly, an intersection of $T_{\rm max}(x)$ and $T_{c1}(x)$ was found to occur right at $x=0.03$,[36] i.e., where $T_{c1}(x)$ attains its maximum value. The maximum structure in $\alpha(T)$ is shown for the various Th concentrations in Fig. 11. For weak Th dopings, i.e., $x=0.01$, 0.017, and 0.022 the maximum progressively grows in size and narrows. At $x=0.03$ the maximum is reduced while its position is found to coincide with the superconducting transition at T_{c1} that manifests itself in the steep drop of $\alpha(T)$ upon cooling. This coincidence at $B=0$ can be demonstrated by applying a field of $B=3$ T that causes a reduction of T_{c1} by more than 0.2 K, cf. Fig. 11. Furthermore, a comparison of the various $B=0$ curves with the corresponding ones taken at $B=2$ T in Fig. 11 indicate a distinct, with x growing field dependence of the low-temperature $\alpha(T)$ behavior. Assuming that the 2 K maximum itself is rather robust against magnetic fields as observed for pure UBe_{13} [see also Ref. 4 for $C(T,B)$ data] and also indicated by the only weakly field-dependent maximum position, it is tempting to attribute the field dependent $\alpha(T)$ contribution to the presence of a finite $\alpha_n<0$ at $B=0$. The small but finite field effect visible in the data for $x=0.01$ suggests that the negative α_n contribution is already

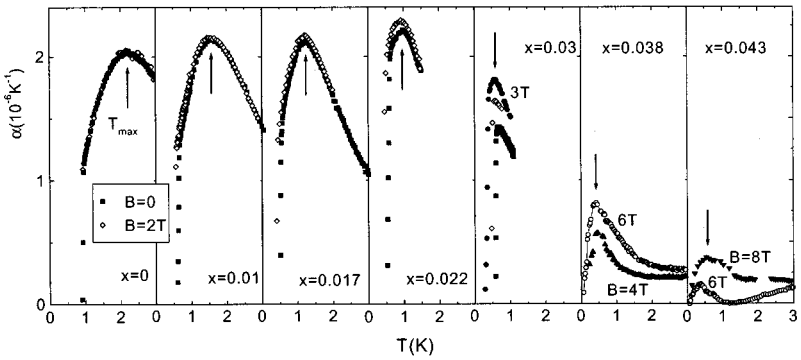

FIG. 11. A section of the low-temperature thermal-expansion data on $U_{1-x}Th_xBe_{13}$ around the peak anomaly at T_{max} for varying x. For $x \leqslant 0.03$, where the peak anomaly is visible already at $B=0$ (■), data at $B=2$ T (◇) [and 3 T (●) for $x=0.03$] are included. A finite field is necessary for $x=0.038$ and 0.043 to make the anomaly visible.

present at this low doping level and that it grows with x, cf. Fig. 11. For $x=0.03$ the negative α_n may be directly seen at temperatures $T_{c1} \leqslant T \leqslant T_{c2}$ where α exhibits a plateau at negative values out of which the transition at T_{c2} emerges, cf. Fig. 2.

As shown in Figs. 4 and 5 for the compounds with $x > 0.03$, there is no maximum structure visible in the $\alpha(T)$ data at $B=0$. Here, the n-state expansivity is governed by the negative α_n contribution that sets in at somewhat elevated temperatures. In finite fields strong enough to substantially reduce this negative contribution, however, a rather small maximum structure can be resolved at low temperatures, cf. Fig. 4 and 11. Unlike the weakly doped systems, $x \leqslant 0.03$, the position of the maxima for $x=0.038$ and 0.043 appears to be affected by the field—an effect which is most likely due to both an energy scale, T_{max}, being already very small for the latter systems as well as the higher fields used in order to make the anomaly visible. To account for this effect in determining T_{max} for these higher concentrations, we employ a linear extrapolation of $T_{max}(B)$ to $B=0$. As demonstrated in Fig. 7, the so-derived temperatures $T_{max}(x)$ for $x > 0.03$ do fall within the experimental uncertainties on the continuation of the linear $T_{max}(x)$ dependence observed for $x \leqslant 0.03$.

From specific-heat[44,45] and resistivity[46,47] studies under pressure it is known that $T_{max}(p)$ shifts to higher temperatures with increasing pressure. Since Th doping causes an increase of the lattice parameter, corresponding to a negative pressure, a reduction of $T_{max}(x)$ as a function of x is expected as a result of the Th-induced expansion of the unit-cell volume. In order to quantify the relative role of the pure volume effect on the $T_{max}(x)$ dependence, we compare in Fig. 12 the shifts in T_{max} caused by the application of pressure to pure UBe_{13} with those induced by Th doping. The room-temperature lattice constants are used as an abscissa. For the thoriated compounds the lattice parameters are known from x-ray-diffraction studies.[16] For the pressure experiments on pure UBe_{13} we convert the pressure values into lattice parameters using the isothermal compressibility $\kappa_T = -V^{-1} \times \partial V/\partial p = 0.97\,(\text{Mbar})^{-1}$.

As clearly demonstrated in Fig. 12 the reduction of $T_{max}(x)$ for the Th-doped compounds is much stronger compared to the shift expected for the pure volume effect. The latter accounts for about 15% of the observed T_{max} reduction. Hence, the dominant effect on $T_{max}(x)$ can be attributed to Th-induced changes in the electronic properties at low temperatures.

V. DISCUSSION

A. On the nature of the phase transition at T_{c2}

Despite the numerous attempts to unravel the nature of the state below the transition at T_{c2} no consensus has been achieved yet. Important early experimental findings include (i) a pronounced peak in the ultrasound attenuation at T_{c2} indicative of a SDW-type ordering below T_{c2} (Ref. 20) that coexists with superconductivity. (ii) A sudden increase in the slope of the lower critical field, B_{c1}, when cooling the sample below T_{c2}.[22] This result has been interpreted to reflect the increase in the Cooper-pair density as a consequence of a second superconducting transition at T_{c2}.[22] It has been suggested by these authors that below T_{c2} additional parts of the Fermi surface participate in the superconducting order parameter. (iii) On the other hand, muon spin rotation measurements revealed that an effective electronic magnetic moment of $10^{-3}\mu_B$ per U atom is formed below T_{c2}.[21]

These seemingly conflicting experimental results have been explained by proposing a superconducting state that

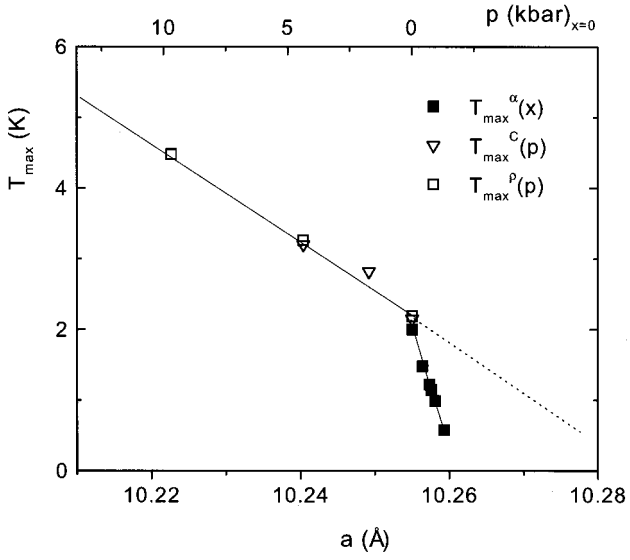

FIG. 12. Variation of the position of the peak anomaly at T_{max} with the lattice parameter. For UBe_{13} the results of pressure studies on the specific heat (Ref. 44) (open triangle) and resistivity (Ref. 47) (open squares) are used, where the pressure values (upper scale) are transformed into lattice constants (lower scale) by means of the isothermal compressibility. Closed squares indicate positions of the thermal-expansion maxima at T^{α}_{max} for the various $U_{1-x}Th_xBe_{13}$ samples investigated ($x \leqslant 0.03$). The lattice parameters were taken from Ref. 16.

breaks time-reversal symmetry and, thus, shows magnetic signatures.[23,25] On the basis of the phase diagram given in Ref. 48 that is similar to the one shown in Fig. 1 except for the line $T_L(x)$ and the curvature of $T_{c2}(x)$, it has been proposed[25] that as a function of x, two different types of (anisotropic) superconductivity cross at $x=x_{c1}\approx 0.019$. As a consequence, the states below T_c for $x<x_{c1}$ and T_{c1} for $x>x_{c1}$ were attributed to single but different representations of the cubic symmetry group while the state below T_{c2} was considered to be a combination of these two representations. Since this state is nonunitary it is expected to generate certain magnetic properties[49] that may explain[25] the experimental observations.

More recent experimental investigations brought to light results that, on the one hand, provide intriguing new details on the T-x phase diagram. On the other hand, in some cases, these results call into question the analysis and interpretation of the above discussed earlier experiments. As an example of the latter, we mention investigations of the vortex dynamics in the mixed state of single crystalline $U_{0.9725}Th_{0.0275}Be_{13}$ by Mota *et al.*[27] The authors find an abrupt increase of the pinning strength upon cooling the system below T_{c2}. Since pinning affects the critical field above which the diamagnetic magnetization of a superconductor exposed to a weak magnetic field departs from a linear field dependence, this abrupt increase of the pinning strength may provide a natural explanation for the observed increase of that experimentally determined critical field [$>B_{c1}$ (Ref. 50)] upon cooling through T_{c2}.

Careful specific-heat measurements on a new generation of $U_{1-x}Th_xBe_{13}$ polycrystals revealed (i) a pronounced peaking of the phase-transition anomaly, ΔC, upon approaching x_{c1} and x_{c2} from outside the two-transition region[16] and (ii) an in-T linear contribution, $C_{\rm lin}=\gamma_{\rm rest}T$, to the low-temperature specific heat in the superconducting state that varies systematically with x.[51] It was argued that both the size and concentration dependence of $\gamma_{\rm rest}$ are consistent with Th acting as resonant scattering centers in an anisotropic superconducting state with gap nodes.[51]

On the other hand, our previous dilatometric investigations on thoriated samples with $x\leqslant 0.03$ provided clear evidence for the existence of an additional line in the T-x phase diagram of $U_{1-x}Th_xBe_{13}$ at $T_L(x)<T_c(x)$ for $x<x_{c1}$.[17] Most importantly, these results demonstrate that $T_L(x)$ for $x<x_{c1}$ marks the precursor of the phase transition at T_{c2} at $x>x_{c1}$, i.e., $T_{c2}(x)$ represents the continuation of $T_L(x)$ at $x>x_{c1}$. It is clear that this finding is incompatible with all scenarios that consider a crossing of two phase transition lines at x_{c1}.[23–25]

Arguments in favor of such a crossing were derived from pressure studies on $T_c(x)$ performed on both sides of x_{c1}.[40] As Fig. 10 clearly demonstrates, however, the variation of $\partial T_c/\partial p$ with x does not support the above proposal of two different superconducting states separated by x_{c1}. For example, the pressure coefficients for $x=0$ and $x=0.0331$ of, respectively, $\partial T_c/\partial p=-13$ mK/kbar and $\partial T_{c1}/\partial p=-14$ mK/kbar are almost identical. The results depicted in Fig. 10 rather suggest that the anomaly in $|\partial T_c(x)/\partial p|$, i.e., the large pressure dependence of T_c in a narrow concentration range is caused by the nearness to x_{c1}.

A new and important piece of information provided by the present work on the nature of the T_{c2} transition is the observation of its close interrelation with the anomalous properties slightly above T_{c2}, i.e., the negative contribution $\alpha_n(T)$ that grows with x. Our data suggest that with increasing x, relative weight of the transition at T_{c2} becomes progressively transferred to this anomalous state above T_{c2}. While a superconducting origin of the negative α_n can be definitely ruled out by our $\chi_{\rm ac}$ measurements, both the sign as well as the strong field dependence of this contribution rather signal a magnetic character.

As for the implications of these new findings for the interpretation of the various phases and phase transitions in the T-x phase diagram of $U_{1-x}Th_xBe_{13}$, we arrive at two possible scenarios both of which imply an intimate interrelation of superconductivity and the symmetry-broken state that forms below T_{c2}. Fundamental to both scenarios is the existence of the line $T_L(x)<T_c(x)$ for $x<x_{c1}$ that evolves into the T_{c2} line for $x>x_{c1}$. Judging from the broad features in $\alpha(T)$ at T_L and the even less pronounced ones in $C(T)$,[17] it appears unlikely that T_L manifests a true phase transition even if allowing for a substantial inhomogeneous broadening.[52] Rather we believe that the shape as well as the sign of the $\alpha(T)$ features indicate short-range correlations most likely of antiferromagnetic nature.[53]

(1) Upon increasing x to above x_{c1} these correlations become long range and $T_{c2}(x)$ manifests a purely antiferromagnetic transition, i.e., a SDW ordering,[20] accompanied by a very small ordered moment of about $10^{-3}\mu_B$. The sizable discontinuity in the specific heat at T_{c2} indicates that a fair fraction of the Fermi surface is involved in the SDW formation. As soon as long-range order has formed at $x>x_{c1}$ the superconducting transition temperature recovers by an as yet unknown reason. One may speculate that the drop in $T_c(x)$ at $x=x_{c1}$ might be the result of critical fluctuations that precede the formation of the long-range ordered state. At a concentration $x=0.03$ at which T_{c1} attains a local maximum, the $T_{c1}(x)$ line intersects with the $T_{\rm max}(x)$ line. The reduction of both $T_{c1}(x)$ as well as the accompanied phase-transition anomalies in $C(T)$ and $\alpha(T)$ upon further increasing x, strongly suggest the onset of a very effective pairbreaking mechanism in this part of the phase diagram (see below). Upon approaching $x_{c2}\approx 0.045$ from inside the critical concentration range, the transition into the superconducting state at T_{c1} becomes gapless, i.e., loses its signatures in $C(T)$ and $\alpha(T)$. With increasing x to above x_{c2}, $T_{c1}(x)$ merges from above in the $T_{c2}(x)$ line at which it becomes ''trapped.''

Though this scenario explains some of the experimental observations, several points remain puzzling:

Does the absence of a linewidth broadening in $B=0$ μSR experiments on both sides of the critical concentration range simply reflect an U moment smaller than $10^{-3}\mu_B$, i.e., too small to be detected?

Why does the long-range antiferromagnetic order at T_{c2} for $x>x_{c2}$ ''trap'' the superconducting transition while the phenomenologically related short-range correlations above T_{c2} leave superconductivity unaffected?

What causes the field dependence of T_{c2} to be so similar to—and on increasing x even approaching—that of T_{c1}?

On the other hand, a purely superconducting transition at T_{c2} would be in conflict with both the broad features at T_L for $x<x_{c1}$ as well as the close interrelation with the short-range (most likely magnetic) phenomena at $T>T_{c2}$. Therefore, we consider as an alternative scenario the possibility of combined magnetic and superconducting order parameters:

(2) The formation of magnetic correlations below the T_L-T_{c2} line is intimately coupled to a second superconducting order parameter. For $x<x_{c1}$ the correlations are short ranged and there is no second superconducting transition in this part of the phase diagram. For $x>x_{c1}$, however, long-range magnetic correlations below T_{c2} go along with a second superconducting transition. As the T_{c1} transition becomes gapless for $x\rightarrow x_{c2}$, the transition seen for $x>x_{c2}$ is then into this combined magnetic superconducting state.

Besides the problem connected with the size of the magnetic moment on both sides of the critical concentration range, this proposal faces the questions:

What causes the intimate coupling of the second superconducting to the magnetic order parameter? Is it the strong tendency towards a SDW formation that is inherent to anisotropic superconducting states?[57] In this case, where the primary order parameter associated with T_{c2} would be of superconducting nature, how do we have to interpret the broad features at $T_L(x)$?

Why do *two* superconducting transitions at T_{c1} and T_{c2} occur? Are they connected to different portions of the Fermi surface?[58] Can these two superconducting order parameters form a combined one below T_{c2} such that the strong pinning effects[27] are explained by dissociation of vortices in domain walls?[29]

B. The second low-energy scale T_{max} and its implication for superconductivity

Besides the characteristic (Kondo) scale T^* of the order 8–25 K,[2,3,43] which accounts for the extremely large effective carrier masses, there exists at least one more low-energy scale in UBe_{13}. The latter manifests itself in a distinct maximum in the coefficient of thermal expansion and a less pronounced shoulder in the specific heat around 2 K.[4,6] At about the same temperature, a distinct maximum shows up in the resistivity as well.[1,42] Remarkably enough, the response observed for the peaks in the resistivity[46,47] and specific heat[44,45] is identical to the application of external pressure (in the pressure range where both quantities have been studied, i.e., $p\leqslant 4.4$ kbar), but is strikingly different to magnetic fields. While the peak in C (and α) has an only very weak field dependence[4] the resistivity maximum is rather sensitive to magnetic fields.[42]

As discussed in Ref. 36 both the positive sign and the shape of the $\alpha(T)$ anomaly at T_{max} are reminiscent of local Kondo-type spin fluctuations. In fact, a crude estimate of the respective contributions to the thermal expansion $\delta\alpha_{2\,K}$ and specific heat $\delta C_{2\,K}=C(x=0)-C(x=0.06)$ as read off the data shown in Ref. 3, yields a corresponding Grüneisen parameter for pure UBe_{13}

$$\Gamma_{2\,K}=\frac{3V_{mol}\delta\alpha_{2\,K}}{\delta C_{2\,K}}$$

of $\Gamma_{2\,K}=100\pm 20$ typical for low-lying Kondo fluctuations.[59,60] Since Γ is related to the volume dependence of the characteristic temperature T_{max} via $\Gamma=-\partial\ln T_{max}/\partial\ln V=\kappa_T {T_{max}}^{-1}\partial T_{max}/\partial p$, it is instructive to compare $\Gamma_{2\,K}$ with this number, i.e., the Grüneisen parameter Γ using the results of pressure studies on the 2 K anomaly. Both resistivity[46,47] as well as specific-heat measurements under hydrostatic-pressure conditions[44,45] yield $\Gamma\approx 110$ in good agreement with the above thermodynamic results.

With increasing Th concentration the characteristic temperature (energy scale) T_{max} becomes linearly suppressed. It was shown that this reduction is predominantly caused by Th-induced changes in the electronic states and to an only minor extent influenced by the accompanied lattice expansion. Investigations in magnetic fields sufficiently strong to suppress both the phase-transition anomalies associated with T_{c1} and T_{c2} as well as the negative α_n above T_{c2} for $x>0.03$ demonstrate that the 2 K anomaly persists in this part of the phase diagram. Its position follows, to a good approximation, the linear $T_{max}(x)$ dependence found for $x<0.03$. Moreover, Fig. 7 suggests that $T_{max}(x)$ terminates at a concentration $x\approx 0.043$ that is very close to x_{c2}. Whether this coincidence is accidental or whether $T_{max}\rightarrow 0$ even marks the second critical concentration remains an interesting question that deserves further investigation.

An interrelation of $T_{max}(x)$ and superconductivity is suggested by the fact that the $T_{c1}(x)$ and $T_{max}(x)$ lines intersect right at $x=0.03$ where T_{c1} attains its maximum. As pointed out in Ref. 36 the reduction of T_{c1} for $x>0.03$ would be compatible with T_{max} representing the characteristic temperature of local Kondo-type spin fluctuations: As long as $T_{max}>T_c$, these fluctuations are to a substantial extent frozen out, i.e., harmless for superconductivity. Once this inequality is reversed at $x=0.03$, i.e., T_{max} has become smaller than T_{c1}, however, these fluctuations represent an effective pair-breaking mechanism which may account for the strong pair-breaking effects found for $x\geqslant 0.038$, i.e., the efficient reduction in $\Delta\alpha_1$ and ΔC_1. The above results are consistent with a two-band scenario where T_{max} has the meaning of a Kondo temperature of ''more localized'' $5f$ states, while $T^*\approx 8-25$ K is the characteristic temperature of the ''less localized'' ones. The latter are the carriers of heavy-fermion superconductivity.

On the other hand, an interpretation of the 2 K anomaly greatly contrasting the one given above has been put forward by Knetsch *et al.*[3] based on the analysis of resistivity measurements. The authors found a strongly nonlinear x dependence of the resistivity maximum T^{ρ}_{max}, which extrapolates into the critical point which marks the local minimum of $T_c(x)$ at $x=x_{c1}$. Based on the location of $T^{\rho}_{max}(x)$ in the T-x phase diagram, this feature was interpreted to represent non-local spin fluctuations that are pair breaking as long as $T^{\rho}_{max}(x)>T_c(x)$. Once $T^{\rho}_{max}(x)$ becomes exceeded by $T_c(x)$ at $x=x_{c1}$, these fluctuations are frozen out allowing $T_{c1}(x)$ to rise.[3]

Although one cannot definitely rule out the existence of *two* distinct low-T scales measured by T^{ρ}_{max} and T^{α}_{max}, which are degenerate at $x=0$ but split off at finite x and have, e.g., to be associated with independent anomalies in the charge and spin channels, the above discrepancy might simply re-

flect difficulties in following the rather small feature at $T^{\rho}_{\max}$ as a function of x. The latter notion is supported by the equivalence of the Grüneisen parameters derived from resistivity measurements at $x=0$ under pressure and from the ambient-pressure thermodynamic results.

VI. CONCLUSION

By means of high-resolution thermal-expansion measurements the low-temperature normal- and superconducting-state properties of $U_{1-x}Th_xUBe_{13}$ have been explored over a wide concentration range $0 \leqslant x \leqslant 0.052$. Owing to the strong coupling of the low-temperature electronic properties to the lattice degrees of freedom that characterizes this system, these studies enabled us to disclose new features in the T-x plane that have been overseen by all other techniques applied to this system so far. Besides a nonmonotonic x dependence of the superconducting transition temperature and the occurrence of a second phase transition as a function of temperature within a certain x range, the substitution of thorium for uranium is found to cause additional anomalies that appear to be intimately related to the irregular points in the T-x phase diagram: The presence of thorium induces an anomaly in the low-T normal state that manifests itself in a negative $\alpha(T)$ contribution α_n. Our analysis indicates a common (presumably magnetic) nature of this feature and the lower of the two subsequent phase transitions at T_{c2} for $x_{c1}<x<x_{c2}$: we propose that α_n is due to the freezing out of short-range correlations above the long-range order below T_{c2}. For $x<0.03$ the low-T normal-state expansivity at $B=0$ is governed by a pronounced maximum at $T_{\max}(x)$ with $T_{\max}(0)=2$ K that, besides $T^* \sim 8-25$ K, marks a second low-energy scale in this system. As we have discussed previously,[36] Th substitution causes a linear reduction of $T_{\max}(x)$ that intercepts with $T_{c1}(x)$ right at $x=0.03$, i.e., where the latter attains its maximum. Our present measurements in magnetic fields indicate that (i) this feature persists also for $x>0.03$ where, in the absence of a field, it is masked by the superconducting transition and (ii) that it follows the linear concentration dependence found for $x<0.03$. The observation that $T_{\max}(x)$ vanishes at $x \approx 0.043$, i.e., almost exactly at x_{c2} suggests a close interrelation of this energy scale with the second irregular point, x_{c2}, in the T-x plane. As for the nature of the various phases and phase-transition lines below the normal- to superconducting-state transition, the present study together with our previous work[17] reveal intriguing new aspects: An anomaly in the superconducting state was found at $T_L<T_c$ for $x<x_{c1}$ that marks the precursor of the transition at T_{c2} for $x>x_{c1}$. As an important consequence, this observation rules out all scenarios that consider the crossing of two different types of (anisotropic) superconducting states at x_{c1}. Rather our data indicate that $T_c(x)$ for $x<x_{c1}$ connects to $T_{c1}(x)$ at x_{c1} and that the corresponding T_c-T_{c1} line stays above the T_L-T_{c2} line. Upon increasing x to above 0.03, the progressive reduction of the phase-transition anomalies at T_{c1} in both thermal expansion $\Delta\alpha_1$ and specific heat ΔC_1 indicate the action of an effective pair-breaking mechanism in this part of the T-x phase diagram that leads to a gapless superconducting state for $x \rightarrow x_{c2}$. As a possible source, we propose local Kondo-type spin fluctuations that manifest themselves in the anomalies at $T_{\max}(x)$. Since at $x=x_{c2}$ the T_{c1} transition has lost its signatures in both $\alpha(T)$ and $C(T)$, the phase-transition anomaly seen for $x>x_{c2}$ has to be associated with the T_{c2} transition. Concomitant measurements of the ac susceptibility indicate that in this part of the phase diagram T_{c2} coincides with the normal- to superconducting-state transition. Whether this coincidence reflects a (gapless) superconducting state (at T_{c1}) that is trapped by an as yet unknown reason by a magnetic phase transition (at T_{c2}), or whether T_{c2} represents a transition into a state characterized by a combined magnetic and (second) superconducting order parameter remains an open question. Further work, in particular from the theoretical side is required to explore the latter possibility in more detail.

ACKNOWLEDGMENTS

Numerous fruitful conversations with P. Thalmeier, E.-W. Scheidt, and M. Tachiki are gratefully acknowledged.

[1] H. R. Ott, H. Rudigier, Z. Fisk, and J. L. Smith, Phys. Rev. Lett. **50**, 1595 (1983).

[2] R. Felten, F. Steglich, G. Weber, H. Rietschel, F. Gompf, B. Renker, and J. Beuers, Europhys. Lett. **2**, 323 (1986).

[3] E. A. Knetsch Ph.D. thesis, University of Leiden, 1993.

[4] H. M. Mayer, U. Rauchschwalbe, C. D. Bredl, F. Steglich, H. Rietschel, H. Schmidt, H. Wühl, and J. Beuers, Phys. Rev. B **33**, 3168 (1986).

[5] A. de Visser, N. H. van Dijk, K. Bakker, J. J. M. Franse, A. Lacerda, J. Flouquet, Z. Fisk, and J. L. Smith, Phys. Rev. B **45**, 2962 (1992).

[6] J. S. Kim and G. R. Stewart, Phys. Rev. B **51**, 16 190 (1995).

[7] J. L. Smith, Z. Fisk, J. O. Willis, B. Batlogg, and H. R. Ott, J. Appl. Phys. **55**, 1996 (1984).

[8] F. Steglich, P. Gegenwart, R. Helfrich, C. Langhammer, P. Hellmann, L. Donnevert, C. Geibel, M. Lang, G. Sparn, W. Assmus, G. R. Stewart, and A. Ochiai, Z. Phys. B: Condens. Matter **103**, 235 (1997).

[9] P. Gegenwart, C. Langhammer, C. Geibel, R. Helfrich, M. Lang, G. Sparn, F. Steglich, S. Horn, L. Donnevert, A. Link, and W. Assmus, Phys. Rev. Lett. **81**, 1501 (1998).

[10] G. Bruls, B. Wolf, D. Finsterbusch, P. Thalmeier, I. Kouroudis, W. Sun, W. Assmus, B. Lüthi, M. Lang, K. Gloos, F. Steglich, and R. Modler, Phys. Rev. Lett. **72**, 1754 (1994).

[11] Besides samples with T_c values between 0.85 and 0.95 K a second variant of UBe_{13} with a markedly lower T_c of 0.75 K has recently been identified. The latter is characterized by distinct differences in both the normal and superconducting state properties (Refs. 12 and 13).

[12] C. Langhammer, R. Helfrich, A. Bach, F. Kromer, M. Lang, T. Michels, M. Deppe, F. Steglich, and G. R. Stewart, J. Magn. Magn. Mater. **177-181**, 443 (1998).

[13] F. Steglich, C. Geibel, R. Helfrich, F. Kromer, M. Lang, G. Sparn, P. Gegenwart, L. Donnevert, C. Langhammer, A. Link, J.

S. Kim, and G. R. Stewart, J. Phys. Chem. Solids **59**, 2190 (1998).
[14] H. R. Ott, H. Rudigier, T. M. Rice, K. Ueda, Z. Fisk, and J. L. Smith, Phys. Rev. Lett. **52**, 1915 (1984).
[15] H. R. Ott, H. Rudigier, Z. Fisk, and J. L. Smith, Phys. Rev. B **31**, 1651 (1985).
[16] E.-W. Scheidt, T. Schreiner, P. Kumar, and G. R. Stewart, Phys. Rev. B **58**, 15 153 (1998).
[17] F. Kromer, R. Helfrich, M. Lang, F. Steglich, C. Langhammer, A. Bach, T. Michels, J. S. Kim, and G. R. Stewart, Phys. Rev. Lett. **81**, 4476 (1998).
[18] R. J. Zieve, D. S. Jin, T. F. Rosenbaum, J. S. Kim, and G. R. Stewart, Phys. Rev. Lett. **72**, 756 (1994).
[19] J. A. Sauls, Adv. Phys. **43**, 113 (1994).
[20] B. Batlogg, D. Bishop, B. Golding, C. M. Varma, Z. Fisk, J. L. Smith, and H. R. Ott, Phys. Rev. Lett. **55**, 1319 (1985).
[21] R. H. Heffner, J. L. Smith, J. O. Willis, P. Birrer, C. Baines, F. N. Gygax, B. Hitti, E. Lippelt, H. R. Ott, A. Schenck, E. A. Knetsch, J. A. Mydosh, and D. E. MacLaughlin, Phys. Rev. Lett. **65**, 2816 (1990).
[22] U. Rauchschwalbe, F. Steglich, G. R. Stewart, A. L. Giorgi, P. Fulde, and K. Maki, Europhys. Lett. **3**, 751 (1987).
[23] R. Joynt, T. M. Rice, and K. Ueda, Phys. Rev. Lett. **56**, 1412 (1986).
[24] P. Kumar and P. Wölfle, Phys. Rev. Lett. **59**, 1954 (1987).
[25] M. Sigrist and T. M. Rice, Phys. Rev. B **39**, 2200 (1989).
[26] R. J. Zieve, T. F. Rosenbaum, J. S. Kim, G. R. Stewart, and M. Sigrist, Phys. Rev. B **51**, 12 041 (1995).
[27] A. C. Mota, E. Dumont, and J. L. Smith, J. Low Temp. Phys. **117**, 1477 (1999).
[28] E.-W. Scheidt, T. Schreiner, and G. R. Stewart, J. Low Temp. Phys. **114**, 115 (1999).
[29] M. Sigrist and D. F. Agterberg, cond-mat/9910526 (unpublished).
[30] H. R. Ott, H. Rudigier, E. Felder, Z. Fisk, and J. L. Smith, Phys. Rev. B **33**, 126 (1986).
[31] M. Lang, Ph.D. thesis, TU Darmstadt, 1991.
[32] G. R. Stewart, Rev. Sci. Instrum. **54**, 1 (1983).
[33] R. Helfrich, Ph.D. thesis, TU Darmstadt, 1998.
[34] D. S. Jin, T. F. Rosenbaum, J. S. Kim, and G. R. Stewart, Phys. Rev. B **49**, 1540 (1994).
[35] T. Schreiner, E.-W. Scheidt, and G. R. Stewart, Solid State Commun. **108**, 53 (1998).
[36] M. Lang, R. Helfrich, F. Kromer, C. Langhammer, F. Steglich, G. R. Stewart, and J. S. Kim, Physica B **259-261**, 608 (1999).
[37] Note that discrepancies in the phase-transition temperatures between specific heat and thermal expansion for $U_{0.962}Th_{0.038}Be_{13}$ may indicate small differences in the actual Th concentration for the two samples studied.
[38] T. Schreiner, E.-W. Scheidt, P. Kumar, and G. R. Stewart, Physica B **259-261**, 625 (1999).
[39] F. Kromer, M. Lang, F. Steglich, J. S. Kim, and G. R. Stewart, Physica B **259-261**, 623 (1999).
[40] S. E. Lambert, Y. Dalichaouch, M. B. Maple, J. L. Smith, and Z. Fisk, Phys. Rev. Lett. **57**, 1619 (1986).
[41] For $x=0.038$ thermal-expansion data of an annealed sample were combined in the Ehrenfest relation with specific-heat results on an unannealed one. Both samples, however, have similar T_{c2} values.
[42] U. Rauchschwalbe, F. Steglich, and H. Rietschel, Europhys. Lett. **1**, 71 (1986).
[43] E. A. Knetsch, G. J. Nieuwenhuys, J. A. Mydosh, R. H. Heffner, and J. L. Smith, Physica B **186-188**, 251 (1993).
[44] N. E. Phillips, R. A. Fisher, J. Flouquet, A. L. Giorgi, J. A. Olsen, and G. R. Stewart, J. Magn. Magn. Mater. **63&64**, 332 (1987).
[45] J. D. Thompson, J. Magn. Magn. Mater. **63&64**, 358 (1987).
[46] J. D. Thompson, M. W. McElfresh, J. O. Willis, Z. Fisk, J. L. Smith, and M. B. Maple, Phys. Rev. B **35**, 48 (1987).
[47] H. A. Borges, J. D. Thompson, A. C. Aronson, J. L. Smith, and Z. Fisk, J. Magn. Magn. Mater. **76-77**, 235 (1988).
[48] H. R. Ott, Helv. Phys. Acta **60**, 62 (1987).
[49] G. E. Volovik and L. P. Gor'kov, Pis'ma Zh. Eksp. Teor. Fiz. **39**, 550 (1984) [JETP Lett. **39**, 674 (1984)]; Zh. Eksp. Teor. Fiz. **88**, 1412 (1985) [Sov. Phys. JETP **61**, 843 (1985)].
[50] This experimentally determined critical field is equivalent to B_{c1} *only* when flux pinning is sufficiently small.
[51] T. Schreiner, E.-W. Scheidt, and G. R. Stewart, Europhys. Lett. **48**, 568 (1999).
[52] For an inhomogeneously broadened transition at $x=0$, there would be no reason why an increase of the thorium (impurity) concentration should cause a continuous sharpening, i.e., a drastic reduction of the inhomogeneities, in the way as observed in our experiment.
[53] In this respect we like to mention thermal-expansion results on polycrystalline $CeAl_3$ (Ref. 54) yielding a negative $\alpha(T)$ anomaly similar to those observed here for small x. These features have been linked to the occurrence of quasistatic frustrated magnetic correlations that develop at low temperatures as observed in μSR experiments (Ref. 55). Unlike the present case, however, indications for a spatially inhomogeneous partly coherent state were found by these studies (Ref. 55). In fact, subsequent measurements on carefully prepared single crystalline material showed that in the strain-released state, $CeAl_3$ exhibits a long-range antiferromagnetic order at somewhat elevated temperatures (Ref. 56).
[54] M. Ribault, A. Benoit, J. Flouquet, and J. Palleau, Phys. Lett. **40A**, L413 (1979).
[55] S. Barth, H. R. Ott, F. N. Gygax, B. Hitti, E. Lippelt, A. Schenck, C. Baines, B. van den Brandt, T. Konter, and S. Mango, Phys. Rev. Lett. **59**, 2991 (1987).
[56] G. Lapertot, R. Calemczuk, C. Marcenat, J. Y. Henry, J. X. Boucherle, J. Flouquet, J. Hammann, R. Cibin, J. Cors, D. Jaccard, and J. Sierro, Physica B **186-188**, 454 (1993).
[57] K. Machida and M. Kato, Phys. Rev. Lett. **58**, 1986 (1987).
[58] K. Takegahara and H. Harima, Physica B **281&282**, 764 (2000).
[59] R. Schefzyk, J. Heibel, F. Steglich, R. Felten, and G. Weber, J. Magn. Magn. Mater. **47&48**, 83 (1985).
[60] A. de Visser, J. J. M. Franse, A. Lacerda, P. Haen, and J. Flouquet, Physica B **163**, 49 (1990).